# Mechanical anisotropy and inhomogeneity of an aromatic liquid crystalline polyester

**J. Sweeney, B. Brew, R. A. Duckett and I. M. Ward***
*IRC in Polymer Science and Technology, University of Leeds, Leeds LS2 9JT, UK*
*(Received 18 October 1991; revised 8 June 1992; accepted 17 July 1992)*

The mechanical anisotropy of injection moulded plaques of a liquid crystalline polymer based on a copolyester of *p*-hydroxybenzoic acid, isophthalic acid and hydroquinone has been studied. The inhomogeneity of the elastic anisotropy has been determined by a combination of static and ultrasonic measurements. The elastic constants are discussed in the light of previous results for anisotropic polymers and are shown to be consistent with an aggregate model to describe the relationship between mechanical anisotropy and molecular orientation.

**(Keywords: liquid crystal; copolyester; mechanical properties; Poisson's ratio; molecular orientation)**

## INTRODUCTION

Liquid crystal polymers (LCPs) which are melt processable have recently attracted a lot of interest. Their potential use in structural applications makes it highly desirable that their elastic properties be known; in addition, such knowledge is useful for the application of fracture mechanics. In the case of injection mouldings, characterization of elastic properties is complicated by their inhomogeneous nature, so that any detailed description must include data on how properties vary from point to point. Such a description, of injection mouldings of a particular LCP, is the subject of this paper.

There have been a number of studies of the structures which can arise in LCPs. Ide and Ophir[1] examined simple flow fields and showed how the observed skin–core structure could develop. Thapar and Bevis[2] reported layered sheet morphology in injection mouldings. Weng *et al.*[3] showed that a skin–core model gave a simplified view of a structure which, when studied on a small scale, revealed a complex hierarchical nature. Another detailed study is due to Sawyer and Jaffe[4]. Some quantitative characterization of the structure of injection mouldings has been achieved using mechanical[5] and X-ray[5,6] measurements.

In this paper, injection mouldings of a development material (manufactured by ICI) are described in terms of their elastic properties. The measurements were motivated in part by the need for data to assist in the interpretation of the fracture behaviour; information about the degree of inhomogeneity is essential and data on the level of anisotropy is desirable. The measurements reported here proved invaluable in a study of fracture which has been reported in a separate publication[7]. The large specimen size required for fracture measurements, together with the desire to examine the fracture of material resembling that used in practice in load bearing applications, were the major factors in the decision to study injection moulded material.

A variety of techniques, both static and dynamic, have been used to measure mechanical properties. The scale and nature of the inhomogeneity is examined and values of all the elastic constants are estimated as a function of position within the moulding thickness.

## EXPERIMENTAL

### *Material*

The material was based on an aromatic copolyester comprising *p*-hydroxybenzoic acid/isophthalic acid/hydroquinone (36:32:32). It was supplied in the form of picture frame injection mouldings (6 mm thick). Other dimensions are given in *Figure 1*. The mouldings were made using a 20 t injection moulding machine (DEMAG W20) with temperature increasing along the barrel from 320 to 335°C at the nozzle end and the mould at 70°C. Polymer was injected at a single point I. In this study, attention is confined to the symmetric regions in the long arms of the moulding, one of which is defined as ABCD in *Figure 1*. The primary interest is the variation in properties through the 6 mm dimension.

A layered structure was visible as light and dark regions of polymer, as noted previously[3]. This was observed by cutting a moulding along EF (see *Figure 1*) and polishing the edge. A photograph of the result is shown in *Figure 2*. The pattern resembles that occurring in injection mouldings of short fibre reinforced thermoplastic[8].

Axes are defined on *Figure 1*, with direction 3 along the mould fill direction (MFD) in the area of interest, direction 1 in the plane of the plaque normal to 3, and direction 2 through the 6 mm plaque thickness.

### *Static measurements*

One class of measurements concerns specimens between 2 mm thick and 6 mm thick in the 2 direction tested in three-point bend. A universal testing machine operating

* To whom correspondence should be addressed

0032-3861/92/234901-07

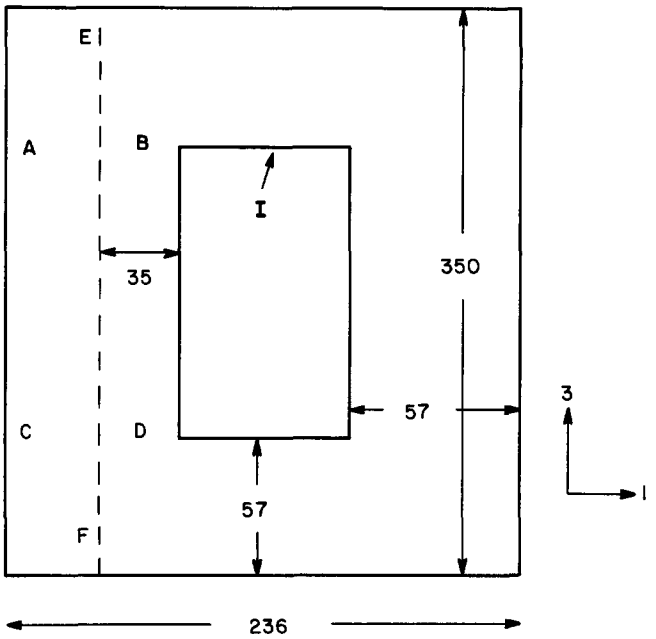


**Figure 1** Dimensions (mm) of injection moulded plaques. Injection point is at I

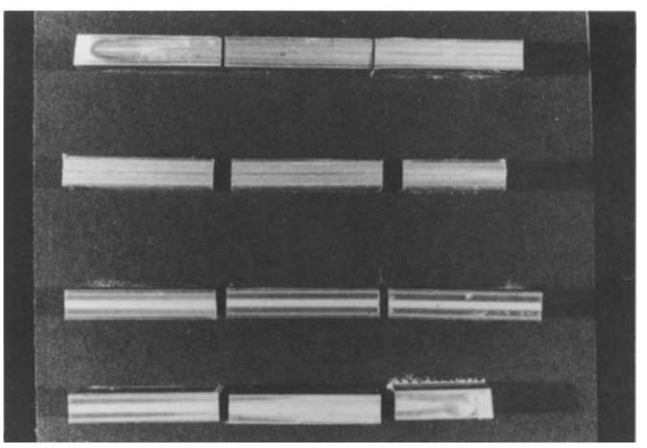

**Figure 2** Polished edge EF of *Figure 1* (E top left, F bottom right) showing layered through-thickness structure

at a speed of 0.5 mm $min^{-1}$ was used to bend specimens as defined in *Figures 3a* and *b*. In these experiments the bending was about either the material 1 axis or 3 axis, giving, respectively, measurements of moduli $E_3$ or $E_1$.

Since the properties vary in the 2 direction, a single experiment gives a value of modulus averaged over the specimen thickness. The averaging is such as to give greater weight to the outer regions of the specimen where the strain is highest, and the values obtained should therefore be treated with caution. However, they serve as a guide to the material stiffness and anisotropy. Results of this nature are given in a later section and are based on specimens as defined in *Figures 3a* and *b*. Those in *Figure 3a* were of the original plaque thickness, with the specimens aligned along the 1 axis tested across a 40 mm span and specimens along the 3 axis tested across a 100 mm span. Those in *Figure 3b* were 5 mm thick, as a result of machining off 0.5 mm layers from each surface. Moduli from these specimens relate to material external to the relatively highly oriented skin region. For the upper set of specimens of *Figure 3b* aligned along the 1 direction, it was possible to test specimens of varying widths in the

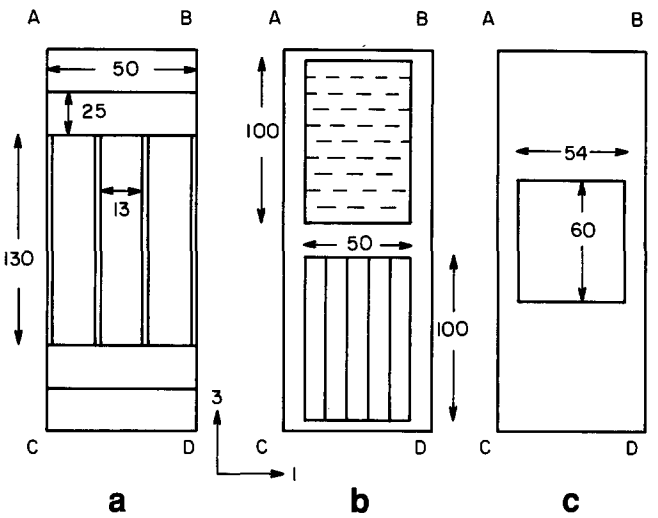


**Figure 3** Positions of specimens within the plaque (region ABCD in *Figure 1*). (a) Bend specimens. Horizontal 50 mm long specimens are of full 6 mm thickness for bending about the 3 axis to give $E_1$. Vertical 130 mm long specimens are used to measure $E_3$ by bending about the 1 axis; they provide results for full 6 mm thickness as well as modulus profiles as the specimen is ground thinner. (b) Bend specimens 5 mm thick, i.e. with 0.5 mm skins removed from each surface. Upper rectangle represents specimens for bending about the 3 axis of width varying from 10 to 100 mm to give data on $E_1$ and $s_{13}$. Lower rectangle specimens are 10 mm wide for bending about the 1 axis to give $E_3$. (c) Ultrasonic specimen (2.5–6 mm thick)

3 direction and thus approach a plane strain value of stiffness $E_1$. A 45 mm span was used for all the *Figure 3b* specimens.

Better definition of modulus as a function of thickness was obtained using a technique of successive bend measurements on specimens machined progressively thinner. It was found that layers 0.1 mm thick could be removed from the surfaces in the 1–3 plane by grinding. The strategy adopted to recover the maximum amount of information was to remove layers from alternate sides with testing after each layer removal. Thus, the first test was on the whole 6 mm section, then a layer was removed from one surface and the resulting 5.9 mm thick specimen tested, then a layer was removed from the opposite surface before testing, and so on, until the thinnest practicable specimen thickness of ~2.0 mm was attained. The specimens were as defined by those aligned along the 3 direction in *Figure 3a*, which were tested by bending across a 100 mm span about the 1 axis. The results are thus for $E_3$ and are presented in a later section.

Much thinner (0.43–0.55 mm) specimens were obtained by peeling material from the surface of the region ABCD (*Figure 1*) of the plaques. Estimates of $E_3$ were obtained by testing in three-point bend about the 1 axis across a 30 mm span, using dead weight loading and measuring the central deflection using a displacement transducer. Specimen widths (1 direction) were in the range 4–10 mm. Narrower specimens of ~0.5 mm in the 1 direction were tested for $E_3$ in tension using a miniature tensile tester[9]. Results from these thin surface specimens were used to establish the scale of the inhomogeneity and are discussed below.

*Ultrasonic measurements*

With this technique the specimen is immersed in water and intercepts a beam of ultrasound. The time taken for pulses to pass through the specimen is measured as the

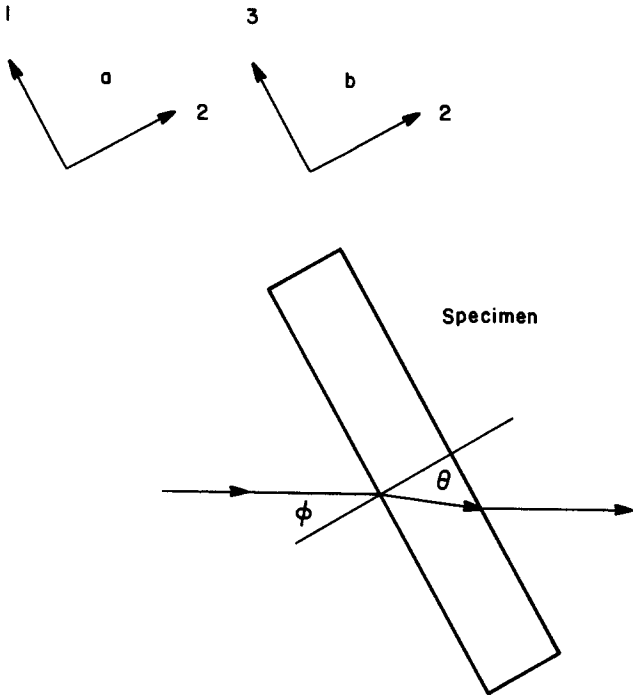


**Figure 4** Path of ultrasonic beam through specimen. The a and b axes sets refer to the two alternative orientations of the specimen

direction of the beam within the specimen is varied and several of the elastic constants can be deduced from a set of measurements. The principles of the method are outlined in reference 10 and the operation of the apparatus used here has been described in references 11 and 12. The specimen is in the form of a rectangular plate which, during the course of the experiment, is rotated about an axis in its plane. The material is assumed to be orthotropic with one of its principal directions coincident with the rotation axis. The beam is in a plane normal to this direction and the problem is one of elasticity in this plane. For a specimen of orthotropic material, rotation can be about two possible axes and so measurements can be made of two such planes. The orientation of the specimen in the beam is shown in *Figure 4*.

A beam of ultrasound of ~13 mm diameter and 2.25 MHz frequency was used. The specimens were taken from the region ABCD (*Figure 1*) of the plaque and were of dimensions as defined in *Figure 3c*. As with the bend measurements, attempts were made to arrive at profiles of the properties by taking measurements on specimens after successive removal of alternate surface layers, in this case of thickness 0.2 mm.

## RESULTS AND DISCUSSION

### *Scale of inhomogeneity*

While the primary interest is the variation in properties in the 2 direction, it is desirable to have some estimate of the scale of the inhomogeneity in the 1–3 plane. This enables the minimum specimen dimension in this plane to be established; properties measured are in effect averages in the 1 and 3 directions and the extent of the specimen needs to be sufficient to give representative values.

The measurements described above of $E_3$ of thin (0.43–0.55 mm) specimens from the plaque surfaces are used for this purpose. Results for bend tests on specimens of widths in the range 4–8 mm in the 1 direction taken from the same plaque are presented in *Figure 5*. Where available, data is included from the 5 mm core of the adjacent material for comparison. There was no systematic dependence of the modulus on specimen thickness, and the distribution of results is characterized by a coefficient of variation of 16%. Much greater variation was observed on specimens narrower in the 1 direction; this was shown by the tests on small specimens using a miniature tensile tester. As an example, specimens ~0.5 mm wide were cut from specimen 4 of *Figure 3* which has modulus of 9.9 GPa, and were found by tensile testing to have moduli in the range 4–22 GPa.

There is also evidence that at greater widths there is less variation. *Figure 6* shows the results from bend tests similar to those above and from the same plaque region, but all with widths in the range 8–10 mm, data from three plaques are included. When the results are normalized to eliminate the variation between plaques, the results are characterized by a coefficient of variation of 11%.

These findings suggest that 10 mm distances in the 1 direction should define a representative area of material. This is consistent with the apparently strong fluctuation in stiffness which occurs at a scale of 0.5 mm.

### *Bend measurements on thick sections*

The apparent moduli $E_1$ and $E_3$ of the whole plaque section were measured using the static methods described above. $E_1$ was in the range 1.8–2.2 GPa and $E_3$ was in

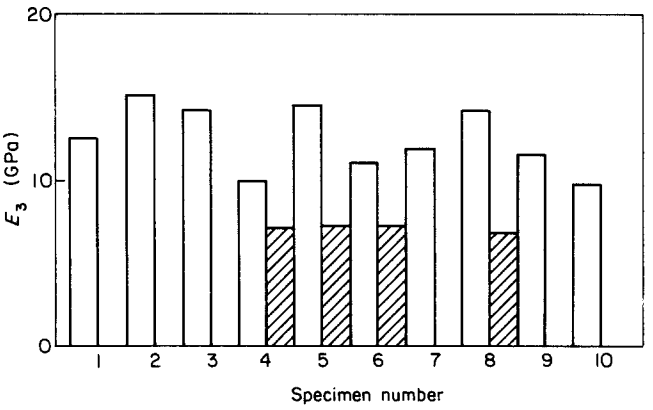


**Figure 5** Moduli of 4–8 mm wide skins (□) along the 3 direction of a plaque. Where available the modulus of the adjacent core materials (▨) is shown for comparison

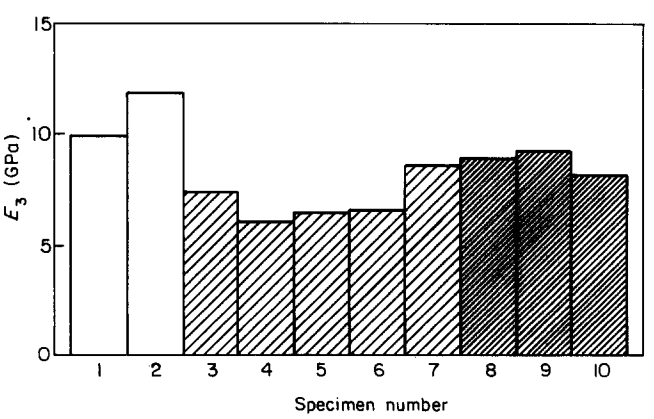


**Figure 6** Moduli 8–10 mm wide skins along the 3 direction: (□) plaque 1; (▨) plaque 2; (▩) plaque 3

the range 11.6–12.7 GPa. No correction has been made for the effect of the average being biased, with greater weight given to the higher strain regions near to the surfaces.

The overall static properties of the material outside the immediate vicinity of the surface were also studied, by bend testing material (5 mm thick) obtained by machining 0.5 mm from both surfaces of the plaque. Values obtained were $E_1 = 2.0 \pm 0.18$ GPa and $E_3 = 8.3 \pm 0.45$ GPa. Measurement of a plane strain value of $E_1$ was made using the same conditions but increasing the specimen width in the 3 direction from 10 to 100 mm; this resulted in an apparent value of $E_1$ increased by 4.9%. This provides a useful check for some of the Poisson's ratio data discussed below.

*Stiffness profiles from bend data*

The procedure by which a series of bend tests was made on specimens ground progressively thinner has been outlined in the Experimental section. Each such bend test yields data in the form of average values of modulus associated with the whole specimen section at each stage of the process. The stiffness profiles (modulus as a function of position within the specimen thickness) were deduced by treating the specimens as assemblies of homogeneous layers and applying beam theory (see Appendix). This ignores the existence of shear stresses which we would expect to act at the interfaces between layers of different modulus; however, finite element modelling of the specimens has shown this effect to be unimportant. In the most extreme cases, the result is that beam theory predicts a negative modulus, whereas the finite element modelling gives instead a very small value of modulus which is effectively zero in comparison with adjacent layers—this is the meaning of the apparently zero regions of modulus in the profiles of *Figures 7* and *8*. The fact that the modulus derived from any layer is very sensitive to changes in the measured overall moduli is a source of difficulty, as experimental error tends to produce large local variations in the profile. This problem was countered by smoothing the input data to remove any fluctuations small enough to be caused by error. However, as a result of this phenomenon it was not possible to make any definite estimates of the degree of error in the final profiles.

The modulus profiles of *Figures 7* and *8* relate to two adjacent specimens aligned along the 3 axis as in *Figure 3a*. The profiles are qualitatively similar, as was that of a third adjacent specimen (not shown here).

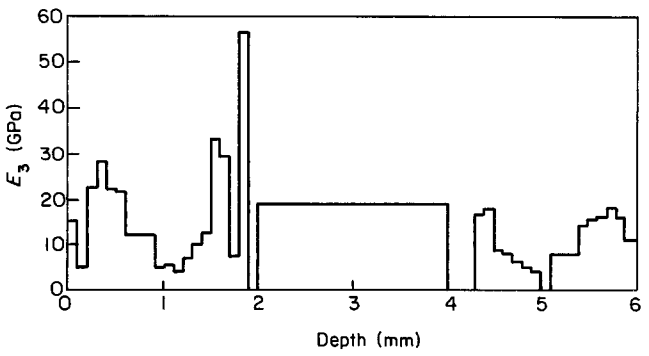


**Figure 7** Profile of $E_3$ through plaque thickness using bend testing (specimens of *Figures 7* and *8* are two adjacent 130 mm long specimens of *Figure 3a*)

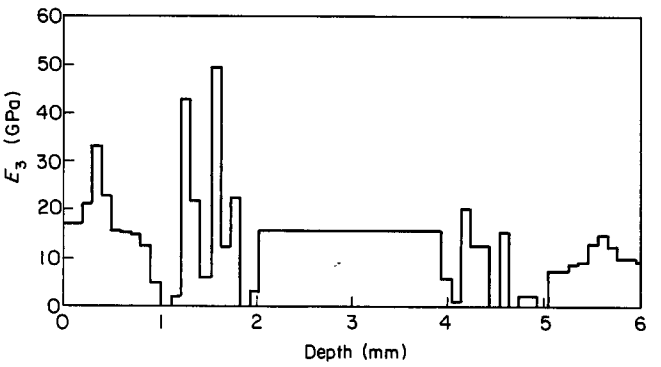


**Figure 8** Profile of $E_3$ through plaque thickness using bend testing (specimens of *Figures 7* and *8* are two adjacent 130 mm long specimens of *Figure 3a*)

Comparison of the two figures provides a guide to the reliability of the results, in view of the difficulty in estimating the errors mentioned above. Very small modulus values occur only at distances $> \sim 0.8$ mm from the surfaces, and there is a tendency for the stiffness to fall off very close ($\sim 0.1$ mm) to the surface; the latter characteristic resembles the orientation profile observed using X-ray techniques[6]. The asymmetry of the profiles about the central plaque surface is also noteworthy; it suggests some asymmetry in the flow fields during injection moulding. Inspection of the gate aperture at the injection point (I in *Figure 1*) revealed that it was not symmetric about the central plane of the moulding, and so could possibly cause such an effect. The single value obtained for the central 2 mm region of the specimens relates to the testing of the thinnest section; it is therefore an average value and subject to the same problem as the tests in the previous section of being biased towards the outer layer stiffnesses. This may explain its high value in comparison with that of the average of the remainder of the profile. Except for the very low regions of the profiles, the moduli are consistent with those obtained by bend testing of thin sections from 3 mm mouldings of this material[13].

*Analysis of ultrasonic measurements*

The experimental method has been described above. The specimens are as defined in *Figure 3c* and in the course of the experiments they are rotated about either the 1 or 3 axis. Equations have been established[10] which relate the stiffnesses $c_{ij}$, the angle of refraction $\theta$ and the ultrasonic velocity $V$ for the case of homogeneous material. Transit time measurements at a series of angles yield data to which these equations can be fitted to give estimates of the $c_{ij}$, as described in reference 11. Rotating the specimen about both its 3 and 1 axes gives information on seven of the nine distinct $c_{ij}$; neither $c_{13}$ nor $c_{55}$ is evaluated and there are two estimates of $c_{22}$.

The above procedure relates to the problem when $\theta$ is both the angle made by the ultrasonic ray with the material 2 axis and the angle of refraction; this condition holds when the principal material directions are parallel with the specimen sides. While we expect this to be approximately the case with the LCP mouldings, we do not assume it but instead introduce an extra free variable $\alpha$ and replace the variable $\theta$ in the equations by $\theta + \alpha$. A value of $\alpha$ is then determined for each experiment along with the $c_{ij}$, and represents the angle which the principal material 2 axis makes with the specimen 2 axis in the 1–2 or 2–3 plane.

The conventional analysis applies to homogeneous material. However, the main condition for the validity of the velocity measurements in this experiment—that the ultrasonic ray which leaves the specimen is parallel to that entering it—is satisfied for a specimen consisting of parallel plane layers of material normal to the specimen 2 axis. Measurements on such a specimen when analysed on the assumption of homogeneity will give average values of the stiffness constants. The form of the average which results from this process is complex; in the simple case of a pulse propagating along the 2 axis of a material consisting of $n$ equal layers the average value of $c_{22}$ is defined by $\langle c_{22} \rangle$:

$$\langle c_{22} \rangle = \left[ (1/n) \sum_{i=1}^{n} (c_{22_i})^{-1/2} \right]^{-2} \quad (1)$$

This form has the desirable property of not being biased towards any particular region of the material, unlike the average obtained using a bend test.

*Ultrasonic results for thick sections*

Ultrasonic measurements were made on a specimen as it was machined progressively thinner from alternate sides as described above. When the results were analysed to give average $c_{ij}$ values associated with the total section thickness of the measured specimen, consistent results were obtained, with good agreement between the two estimates of $c_{22}$ obtained for the 1–2 and 2–3 planes; the $\alpha$ angles between the principal material directions and the specimen axes were small, with a mean value of 3°. The stiffness data obtained using two specimens are given in *Table 1* for three specimen thicknesses corresponding to the whole section, the section with 0.5 mm surface layers removed, and a central region of thickness of 2.3 or 2.5 mm. In addition, engineering constants are given in *Table 2*. These were obtained by inverting the $c_{ij}$ matrix to give compliances $s_{ij}$ on the assumption that $s_{13} = s_{23}$.

The need, when inverting the $c_{ij}$ matrix, for an assumption such as $s_{13} = s_{23}$ arises from the lack of data on $c_{13}$. Alternative assumptions, most obviously $c_{13} = c_{23}$ and Poisson's ratio $\nu_{31} = \nu_{32}$, are possible. The different calculation methods will in general give different results for $s_{13}$, and after comparison with independent estimates of $s_{13}$ we concluded that the condition $s_{13} = s_{23}$ gave good consistency. The independent estimates were made using bend tests, bending about the 3 axis specimens of varying width in the 3 direction as described above, together with three-dimensional finite element (PAFEC) analysis of the bending beam.

The values of $E_1$ and $E_2$ are greater than the values of $E_1$ obtained mechanically and reported above; this is the expected effect of frequency. The values of the Poisson's ratios given in *Table 2* agree well with those of Chivers and Moore[14]. They are also similar to values reported for oriented polyethylene and polypropylene[15].

*Profiles of properties from ultrasonic data*

Results from successive experiments were compared to obtain the pulse transit times for the layer of material which had been removed. When these results were analysed, however, there was often a lack of consistency between the two $c_{22}$ values associated with the 1–2 and 2–3 planes and in some cases the minimization procedure failed. This we attribute to the large percentage errors in the transit times calculated for the removed layers. Since the layers removed were thin (0.2 mm), the associated transit times are differences between experimental transit times of similar size; the size of these differences is comparable with the uncertainty in the transit time measurement.

More consistent data can be derived by analysing the transit time for thicker subregions of the specimen by comparing experimental specimens separated by more than one machining step; the subregion of interest is then two separate layers on either side of the specimen midplane, owing to the strategy of machining alternate sides of the specimen. The values of $c_{ij}$ derived are then averages over two distinct layers of material. A profile of properties built of layers of different thicknesses may be distorted by the effect that thicker layers will be associated with averages over a greater volume of material and so will tend to give stiffnesses closer to those of the average section.

A second method of attacking this problem is to change the angular variation of the pulse transit times for a layer by replacing it with an angular variation associated with total specimen section. A combination of this technique and that outlined above has been used to provide the modulus profiles for specimen 1 in *Tables 1* and *2*. *Figures 9* and *10* give the results for normal and shear moduli.

**Table 1** Stiffness constants (in GPa)

| Section (mm) | Specimen | $c_{11}$ | $c_{22}$ | $c_{33}$ | $c_{12}$ | $c_{23}$ | $c_{44}$ | $c_{66}$ |
|---|---|---|---|---|---|---|---|---|
| 6 | 1 | 7.60 | 6.99 | 15.83 | 5.52 | 5.53 | 1.78 | 0.91 |
| 6 | 2 | 7.21 | 6.71 | 21.64 | 5.28 | 5.95 | 1.43 | 0.82 |
| 5 | 1 | 7.84 | 7.04 | 14.57 | 5.60 | 5.52 | 1.56 | 0.94 |
| 5 | 2 | 7.55 | 6.85 | 20.52 | 5.43 | 5.90 | 1.46 | 0.80 |
| 2.5 | 1 | 8.61 | 7.10 | 13.59 | 5.69 | 5.51 | 1.18 | 1.00 |
| 2.3 | 2 | 7.80 | 6.54 | 21.30 | 5.10 | 6.23 | 1.50 | 0.68 |

**Table 2** Engineering constants (moduli in GPa)

| Section (mm) | Specimen | $E_1$ | $E_2$ | $E_3$ | $\nu_{13}$ | $\nu_{32}$ | $\nu_{21}$ | $G_{12}$ | $G_{23}$ |
|---|---|---|---|---|---|---|---|---|---|
| 6 | 1 | 3.06 | 2.83 | 10.83 | 0.442 | 0.115 | 0.691 | 0.91 | 1.78 |
| 6 | 2 | 2.92 | 2.73 | 15.63 | 0.500 | 0.087 | 0.705 | 0.82 | 1.43 |
| 5 | 1 | 3.18 | 2.87 | 9.62 | 0.442 | 0.132 | 0.682 | 0.94 | 1.56 |
| 5 | 2 | 3.08 | 2.80 | 14.71 | 0.485 | 0.092 | 0.708 | 0.80 | 1.46 |
| 2.5 | 1 | 3.72 | 3.11 | 8.55 | 0.427 | 0.155 | 0.658 | 1.00 | 1.18 |
| 2.3 | 2 | 3.53 | 2.99 | 14.27 | 0.542 | 0.114 | 0.654 | 0.680 | 1.50 |

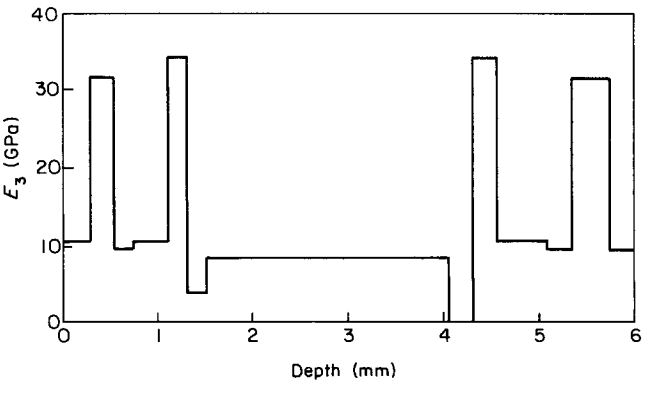


**Figure 9** Profile of $E_3$ through plaque thickness by ultrasonic measurement

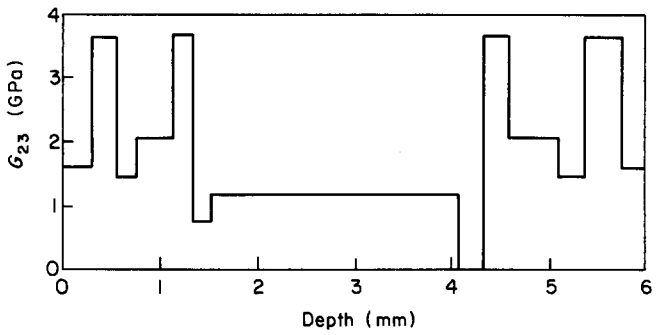


**Figure 10** Profile of $G_{23}$ through plaque thickness by ultrasonic measurement

*Figure 9* gives values for $E_3$ only since the variation in $E_1$ and $E_2$ was small and probably not significant compared with the error in the final results. On the same grounds, shear modulus values, $G_{12}$ values, are excluded from *Figure 10*. In general, the ultrasonic profiles are at a coarser resolution in layer thickness than those obtained mechanically for $E_3$ in *Figures 7* and *8*, and this would account for the lack of high $E_3$ values in *Figure 9*—averaging over a greater thickness masks the extreme values of stiffness. The pattern of behaviour near to the surfaces is similar for $E_3$ in both the mechanical and ultrasonic measurements.

The calculated values of Poisson's ratio varied rapidly and unsystematically through the specimen thickness and are subject to greater uncertainty than the moduli. The ratios associated with the 1–2 plane did, however, show a systematic increase with $E_3$. This can be interpreted as the approach to the ideal condition of zero compliance in the 3 direction ensuring, by conservation of material volume, a constancy of area in the 1–2 plane, and a $\nu_{12}$ or $\nu_{21}$ equal to unity. The results are shown in *Figure 11* where the geometric mean $(\nu_{21}\nu_{12})^{1/2}$ is plotted against $E_3$.

*Interpretation of elastic measurements*

The elastic constants which have been obtained are compatible with previous data for oriented LCPs, and are reasonable on physical grounds. First, the most highly oriented section gives $E_3 > E_1 \sim E_2$, consistent with the known and expected differences between the stiffness in the chain axis direction, which will contribute to $E_3$, compared with $E_1$ and $E_2$ where the stiffness is associated with dispersive forces. The Poisson's ratio $\nu_{13}$ is $\sim 0.5$, which is not unreasonable, and shows that there is only a small volume contraction for stress applied along the 3 direction. On the other hand, $\nu_{21}$ is $\sim 0.7$, which can be anticipated where application of stress in the 1 direction causes only a small deformation in the 3 direction (because this direction is very stiff) and we approach the condition that all the contraction is accommodated in the 1–2 plane and its area is conserved. The shear moduli $G_{23}$ are low at $\sim 1$ GPa which is well-known for these materials[16] and in fibre form leads to low compressive strength.

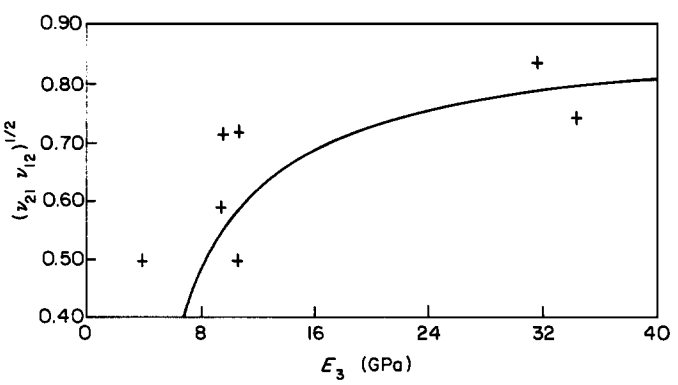


**Figure 11** Poisson's ratios in the 1–2 plane: (+) experiment; (—) aggregate model

In summary, the elastic constants are comparable to those obtained for conventional oriented synthetic fibres such as poly(ethylene terephthalate) or nylon[17], and are similar to many other polymers given a suitable level of orientation. The anisotropy of Poisson's ratio is similar to that in polyethylene and polypropylene monofilaments; it is that expected of a structure akin to material reinforced along the 3 direction with stiff fibres which are prone to shearing parallel to their lengths. The injection mouldings are however of much lower overall molecular orientation than is observed in highly oriented fibres and tapes of LCPs[17]. It is therefore of some interest to discuss the mechanical anisotropy in the light of the aggregate model, which has been used previously for these materials by Blundell *et al.*[6] and Green *et al.*[18].

The plausibility and self-consistency of the results obtained in this section can be discussed with reference to the aggregate model consisting of an assembly of transversely isotropic subunits. The subunits are assumed to be identical and aligned with a distribution of angles with respect to the material 3 axis, so that the overall material anisotropy is less than that of the individual subunit. We adopt the Reuss average as in previous work[6]. The material compliances $s_{ij}$ are then given in terms of the subunit compliances $S_{ij}$ by the relations of reference 15. For instance, $s_{11}$ is given by:

$$s_{11} = (3I_2 + 2I_5 + 3)S_{11}/8 + (3I_3 + I_4)S_{13}/4 + 3I_1 S_{33}/8 + (3I_3 + I_4)S_{44}/8 \quad (2)$$

The subscripts $i$ and $j$ of the subunit properties $S_{ij}$ refer to axes local to the subunit. The $I_i$ are the orientation functions defined by:

$$I_1 = \langle \sin^4 \chi \rangle$$
$$I_2 = \langle \cos^4 \chi \rangle$$
$$I_3 = \langle \sin^2 \chi \cos^2 \chi \rangle$$
$$I_4 = \langle \sin^2 \chi \rangle$$
$$I_5 = \langle \cos^2 \chi \rangle$$

where $\chi$ is the angle which the subunit symmetry axis makes with the material 3 axis and the angled brackets denote the average.

We first derive properties of the subunit which are consistent with the measured values for the average properties of the 5 mm core region, corresponding to the static values for the normal moduli and the ultrasonic values for the Poisson's ratios and shear modulus. As a first step, we assume that the value of $S_{33}$ corresponds to the highest value of $s_{33}$ obtained in the bend test profiles; thus, $S_{33} = 0.0143\,\text{GPa}^{-1}$ corresponding to a modulus of 70 GPa. Similarly, $S_{12}$ is assumed to correspond to the highest value obtained for $\nu_{21}$ (0.84). Other guessed values are used together with the observed value of $s_{33}$ in equation (2) to give an initial estimate of the average angle $\chi$; this value is then used in the other equations to give predictions for the other $s_{ij}$. The

**Table 3** Subunit properties and Reuss averages (in $GPa^{-1}$)

| | $S_{11}$ | $S_{33}$ | $S_{12}$ | $S_{13}$ | $S_{44}$ |
|---|---|---|---|---|---|
| Subunit | 0.50 | 0.0143 | −0.42 | −0.01 | 0.80 |
| | $s_{11}$ | $s_{33}$ | $s_{12}$ | $s_{13}$ | $s_{44}$ |
| Reuss | 0.48 | 0.125 | −0.36 | −0.06 | 0.79 |
| Observed | 0.50 | 0.12 | −0.35 | −0.06 | 1.04 |

calculations are greatly simplified as a result of the assumption that $\chi$ has a single value rather than a distribution of values, so that the orientation vector of each subunit lies along a cone of constant angle; this first order approximation is considered adequate here. An iterative process results in a set of values for the $S_{ij}$ together with an angle $\chi$ which is consistent with the observed $s_{ij}$. Such a set is given in *Table 3*, together with the predicted values for $s_{ij}$ at the calculated average value of $\chi$ of 23.3°.

The Reuss values of $S_{ij}$ in *Table 3* are consistent with the average values for the central 5 mm section of the moulding discussed above, when static measurements are used to define the normal moduli and ultrasonic measurements for the Poisson's ratios; these averages are the 'observed' values in *Table 3*. The model can also be used with a varying $\chi$ to generate relationships between the various elastic properties as the orientation changes. In particular, equations (2) and (3) can be evaluated to model the increase in $\nu_{21}$ as the orientation, and therefore $E_3$, increases. Such a prediction is given in *Figure 11* for comparison with the observed Poisson's ratio in the 1–2 plane as a function of $E_3$. The experimental results are the property profiles obtained using the ultrasonic method. The observed increase in Poisson's ratio is adequately represented and consistent with the aggregate model.

## CONCLUSIONS

The LCP mouldings show rapid variation of mechanical properties in the plane of the mouldings, but representative average properties are obtainable from specimens of ~10 mm in this plane. Overall elastic properties show an anisotropy in stiffness along and across the MFD of a factor of 4–6. Profiles through the plaque thickness of properties can be measured by mechanical or ultrasonic methods using a technique of layering. Skin–core and other structures are observed, with moduli up to 70 MPa. The ultrasonic technique gives useful values of bulk properties for thick layers of material and its main strength is that it gives access to many parameters including the Poisson's ratios. A Reuss average aggregate model is consistent with the experimental observations.

## ACKNOWLEDGEMENTS

This work results from a collaborative project funded by and in collaboration with ICI. We wish to acknowledge the financial support and to thank our colleagues at ICI, Wilton for their participation and many useful suggestions.

## REFERENCES

1 Ide, Y. and Ophir, Z. *Polym. Eng. Sci.* 1983, **23**, 261
2 Thapar, H. and Bevis, M. J. *J. Mater. Sci. Lett.* 1983, **2**, 733
3 Weng, T., Hiltner, A. and Baer, E. *J. Mater. Sci.* 1986, **21**, 744
4 Sawyer, L. C. and Jaffe, M. *J. Mater. Sci.* 1986, **21**, 1897
5 Thapar, H. and Bevis, M. J. *Plastics Rubber Process. Appl.* 1989, **12**, 39
6 Blundell, D. J., Chivers, R. A., Curson, A. D., Love, J. C. and MacDonald, W. A. *Polymer* 1988, **29**, 1459
7 Sweeney, J., Brew, B., Duckett, R. A. and Ward, I. M. *J. Mater. Sci.* 1992, **27**, 3969
8 Folkes, M. J. 'Short Fibre Reinforced Thermoplastics', Wiley, New York, 1982
9 Marsh, D. M. *J. Sci. Instr.* 1961, **38**, 229
10 Read, B. E. and Dean, G. D. 'The Determination of the Dynamic Properties of Polymers and Composites', Adam Hilger Ltd, Bristol, 1978
11 Lord, D. *PhD Thesis* University of Leeds, 1989
12 Dyer, S. R. A., Lord, D., Duckett, R. A., Ward, I. M. and Hutchinson, I. J. *Phys. D.* 1992, **25**, 66
13 Tomlinson, W. J. and Morton, P. E. *J. Mater. Sci. Lett.* 1991, **10**, 154
14 Chivers, R. A. and Moore, D. R. *Polymer* 1991, **32**, 2190
15 Ward, I. M. 'Mechanical Properties of Solid Polymers', 2nd Edn, Wiley, New York, 1990
16 Green, D. I., Davies, G. R. and Ward, I. M. to be published
17 Troughton, M. J., Unwin, A. P., Davies, G. R. and Ward, I. M. *Polymer* 1988, **29**, 1389
18 Green, D. I., Unwin, A. P., Davies, G. R. and Ward, I. M. *Polymer* 1990, **31**, 579

## APPENDIX

### *Beam theory formulation*

A beam specimen is modelled as an assemblage of laminae of different thickness and modulus. The beam theory assumptions of a one-dimensional structure and no shear stresses are made. Then, if there are $n$ layers with the $i$th layer of thickness $d_i$ and modulus $E_i$, equilibrium along the beam direction ensures that:

$$0=\sum_{i=1}^{n} E_i \int_0^{d_i} [\varepsilon_i+(\varepsilon_{i+1}-\varepsilon_i)y/d_i]\,dy \qquad \text{(A1)}$$

where the strains at the boundaries of the $i$th layer are $\varepsilon_i$ and $\varepsilon_{i+1}$. In three-point bend with a total force $P$ and span $I$, equating bending moments gives:

$$PI=4\sum_{i=1}^{n} E_i \int_0^{d_i} [\varepsilon_i(y+D_i)+(\varepsilon_{i+1}-\varepsilon_i)y(y+D_i)/d_i]\,dy \qquad \text{(A2)}$$

where

$$D_i=\sum_{j=1}^{i-1} d_j$$

Finally, the strain gradients in each layer are equated:

$$(\varepsilon_{i+1}-\varepsilon_i)/d_i=(\varepsilon_i-\varepsilon_{i-1})/d_{i-1} \qquad (i=2,\ldots,n) \text{ (A3)}$$

The relations (A1), (A2) and (A3) give a set of $(n+1)$ equations. In principle, they could be solved to give all the strains $\varepsilon_i$ given the values of modulus $E_i$. In practice, the equations are solved with one of the $E_i$ values unknown but with a known relationship between the strains $\varepsilon_1$ and $\varepsilon_{n+1}$ on the surfaces of the beam specimen; this relationship is provided by equating the observed strain on the specimen with the quantity $(\varepsilon_1-\varepsilon_{n+1})/2$.